Cyclin-like Accumulation and Loss of the Putative Kinetochore Motor CENP-E Results from Coupling Continuous Synthesis with Specific Degradation at the End of Mitosis

Kevin D. Brown,* Richard M. R. Coulson,* Tim J. Yen,‡ and Don W. Cleveland*

*Department of Biological Chemistry, Johns Hopkins University School of Medicine, Baltimore, Maryland 21205; and ‡Fox-Chase Cancer Institute, Philadelphia, Pennsylvania 19111

Abstract. CENP-E is a kinesin-like protein that binds to kinetochores through the early stages of mitosis, but after initiation of anaphase, it relocalizes to the overlapping microtubules in the midzone, ultimately concentrating in the developing midbody. By immunoblotting of cells separated at various positions in the cell cycle using centrifugal elutriation, we show that CENP-E levels increase progressively across the cycle peaking at ~22,000 molecules/cell early in mitosis, followed by an abrupt (>10 fold) loss at the end of mitosis. Pulse-labeling with [^{35}S]methionine reveals that beyond a twofold increase in synthesis between G1 and G2, interphase accumulation results primarily from stabilization of CENP-E during S and G2. Despite localizing in the midbody during normal cell division, CENP-E loss at the end of mitosis is independent of cytokinesis, since complete blockage of division with cytochalasin has no affect on CENP-E loss at the M/G1 transition. Thus, like mitotic cyclins, CENP-E accumulation peaks before cell division, and it is specifically degraded at the end of mitosis. However, CENP-E degradation kinetically follows proteolysis of cyclin B in anaphase. Combined with cyclin A destruction before the end of metaphase, degradation of as yet unidentified components at the metaphase/anaphase transition, and cyclin B degradation at or after the anaphase transition, CENP-E destruction defines a fourth point in a mitotic cascade of timed proteolysis.

During mitosis, mammalian cells undertake a complex series of steps that ultimately result in the segregation of chromosomes. The start of mitosis, termed prophase, is marked by initiation of chromosome condensation. At prometaphase, condensation is largely completed, and the nuclear envelope disintegrates. Coordinately, the cytoplasmic microtubule array is disassembled and astral microtubules appear at the separated mitotic poles (centrosomes). Chromosome movements are mediated by microtubules (e.g., Gorbsky et al., 1987; Koshland et al., 1988) that extend from the centrosomes to a specialized region of the chromosome referred to as the kinetochore (Euteneur and McIntosh, 1981). In fact, kinetochores have been shown in vitro to capture microtubules that originate from the spindle poles (Mitchison and Kirschner, 1985). The role of the kinetochore is not a static one, however, since in vivo efforts have shown it to participate actively in poleward chromosome movement (Nicklas, 1989; Reider and Alexander, 1990). Moreover, in vitro experiments (Hyman and Mitchison, 1991) have shown that isolated chromosomes can translocate along microtubules in either direction depending on ATP concentration and inhibition of phosphatases. These observations have lead to the view that the kinetochore plays an active role in chromosomal segregation during mitosis.

Only a handful of mammalian kinetochore antigens have been identified to date. One of these, CENP-E, colocalizes with the centromere/kinetochore during metaphase, but releases from the centromere at, or just after, the onset of anaphase, relocalizing to the midbody during telophase (Yen et al., 1991). cDNA cloning of CENP-E has revealed the 312-kD CENP-E polypeptide to consist of a tripartite structure comprised of amino- and carboxy-terminal globular domains separated by a 1,500-residue α-helical domain that is predicted to form coiled-coils (Yen et al., 1992). Additionally, the amino-terminal domain of CENP-E contains striking homology to the microtubule-dependent motor protein kinesin, demonstrating CENP-E to be a member of the growing family of kinesin-like proteins (for review see Endow, 1991; Skoufias and Scholey, 1993).

Beyond the potential that CENP-E may function as a

Address correspondence to Dr. Don W. Cleveland, Department of Biological Chemistry, Johns Hopkins University School of Medicine, 725 North Wolfe Street, Baltimore, MD 21205.

The present address for Richard M. R. Coulson is Department of Pathology, University of Cambridge, Tennis Court Road, Cambridge CB21QP, England.

kinetochore motor during the early part of mitosis, interest in CENP-E also arose from its cell cycle–dependent accumulation and loss. First suggested by the failure of immunofluorescence methods to detect CENP-E in most interphase cells (Yen et al., 1991), immunoprecipitations of CENP-E from extracts of drug-synchronized HeLa cells at different stages of the cell cycle confirmed that CENP-E levels were low in G1 cell extratcs but increased in amount in extracts derived from S and G2/M cell populations. Furthermore, a qualitative pulse-chase experiment determined that CENP-E was lost as cells transitioned from M phase to G1 (Yen et al., 1992).

The best understood group of proteins whose abundance changes markedly under cell cycle control are the mitotic cyclins A and B. In particular, cyclin B has been shown to peak in abundance before mitosis, but then is nearly quantitatively (~20-fold) lost at the completion of cell division (Evans et al., 1983; Standart et al., 1987; Pines and Hunter, 1989; Westendorf et al., 1989, Hunt et al., 1992). The association of cyclin with the kinase $p34^{CDC2}$ is one of the necessary steps in the formation of maturation promotion factor, a mitotically active kinase complex whose activity is responsible for the transition of interphase cells into mitosis (for review see Murray and Kirschner, 1989*a*; Norbury and Nurse, 1992). The importance of cyclin accumulation and degradation in the control of M-phase initiation and completion is underscored by the observations that the accumulation of cyclins is required for cellular entry into mitosis (Swenson et al., 1986; Minshull et al., 1989*a*; Murray and Kirschner, 1989*b*) and cyclin mutants that cannot be degraded after the onset of mitosis cause cell cycle arrest in mitosis (Murray et al., 1989; Luca et al., 1991; Gallant and Nigg, 1992; van der Velden and Lohka, 1993). While it is now clear that the degradation of cyclin B is not responsible for triggering the metaphase to anaphase transition (Surana et al., 1993; Holloway et al., 1993), as had long been assumed (e.g., Murray and Kirschner, 1989*a*), it seems inescapable that control of cyclin levels serves an important role in the regulation of maturation promotion factor activity.

Following what is known for mitotic cyclins, we now investigate the mechanism(s) responsible for CENP-E accumulation and loss throughout the cell cycle. A combination of approaches reveal that CENP-E is synthesized steadily, but the major contributor to accumulation is stabilization of the polypeptide during S and G2 phases of the cell cycle and rapid, specific degradation at the end of mitosis. The degradation of CENP-E temporally follows that of cyclin B, establishing a temporal cascade of proteolysis during mitosis beginning with cyclin A at or before metaphase, one or more unknown proteins at the metaphase/anaphase transition, cyclin B during or after the metaphase/anaphase transition, and CENP-E later in anaphase/telophase.

Materials and Methods

Cell Culture and Synchronization

HeLa cells were cultured in DME supplemented with 10% FCS. K562 cells were grown in spinner flasks in RPMI 1640 supplemented with 10% calf serum. Both cell lines were maintained at 37°C in a humidified 5% CO_2 atmosphere. The insect cell line (Sf9 cells) that was used for baculovirus expression was maintained at room temperature in Grace's modified insect media supplemented with 10% heat-inactivated FCS.

For centrifugal elutriations, K562 cells were grown to a density of 1-3 $\times 10^5$ cells/ml. Typically, $\sim 3 \times 10^8$ cells were used in each elutriation. Cells were elutriated into 100-ml fractions using a counterflow centrifugal elutriator (JE-63; Beckman Instruments, Inc., Fullerton, CA) according to established protocols (Kauffman et al., 1990). Cell cycle phases were determined by flow cytometry using ethidium bromide (Sherley and Kelly, 1988).

To obtain K562 cells blocked in the G1/S portion of the cell cycle, a double-thymidine block was used. Briefly, thymidine (2 mM final concentration) was added to cultures of cells in exponential growth phase, and the cells were incubated for 24 h. After this period, the cells were harvested by centrifugation, rinsed in thymidine-free complete media, and incubated for an additional 12 h. Subsequently, thymidine was again added to the culture media, and the cells were incubated in this state for an additional 24 h. At the conclusion of this final incubation, flow cytometry analysis determined that >90% of the cell population were synchronized at G1/S.

Mitotic shake off was used for isolation of mitotic HeLa cells. Initially, flasks of HeLa cells in log phase growth were firmly shaken to remove the loosely adherent mitotic cells. Subsequently, the media was decanted, and the cells were harvested by centrifugation (direct observation revealed that >95% of the cells were in mitosis). To obtain cells in early G1, mitotic cells were replated in prewarmed, complete media and incubated for 3 h, after which >97% of the cells were in interphase, as determined by phase-contrast microscopy. Cells blocked in prometaphase were obtained by adding 0.1 μg/ml of nocodazole (prepared as a 1 mg/ml stock solution in ethanol) to cultures of cells from which mitotic cells had been removed by mitotic shake off. After 2 h, blocked cells were harvested by mitotic shake-off and were subsequently replated in prewarmed complete media supplemented with the indicated drug. Stock solutions of cytochalasin D (5 mg/ml) and colchicine (1 mM) were prepared in DMSO and ethanol (100%), respectively.

Electrophoresis and Immunoblotting

Cells were harvested by centrifugation after scraping the culture dish (if necessary). The cell pellets were then rinsed twice in cold (4°C) PBS and lysed by the addition of SDS solubilization solution (50 mM Tris-HCl, pH 7.5, 5 mM EDTA, 1% SDS). The extracts were then placed in a boiling water bath for 5 min, briefly sonicated, and centrifuged to remove the residual insoluble material. The supernatants were removed and stored at −80°C. Protein concentrations were determined by the bicinchonic acid method using bovine albumin as the standard (Smith et al., 1985). Before electrophoresis, extracts were diluted with 3× SDS-sample buffer (150 mM Tris-HCl, pH 6.8, 10% β-mercaptoethanol, 20% glycerol, 3% SDS) and boiled for ~2 min.

SDS-PAGE was carried out according to the protocol of Laemmli (1970). To visualize total protein content, gels were stained for 1 h with Coomassie brilliant blue R-250 (0.1% in 50% methanol, 10% acetic acid). The gels were then destained in 10% methanol, 10% acetic acid overnight.

For immunoblot analysis, gels were electrically transferred (Towbin et al., 1979) to polyvinyldifluoride sheets (Immobilon-P; Millipore Corp., Bedford, MA) for 16 h at 4°C and 150 mA. Sheets were blocked for 1 h in a solution of 5% nonfat dry milk in Tris-buffered saline (10 mM Tris-HCl, pH 7.2, 0.9% NaCl, 0.1% Tween-20), followed by incubation in an appropriate dilution of either the anti-CENP-E antiserum pAbl (Yen et al., 1992), anti-cyclin B antiserum (Muschel et al., 1993), or the anti-α-tubulin monoclonal antibody DM1A (Blose et al., 1984). Immunoreactive bands were visualized with ^{125}I-conjugated-protein A followed by autoradiography on film (XAR; Eastman Kodak, Rochester, NY) for 8–24 h at −80°C with intensifying screens.

Metabolic Labeling and Immunoprecipitation

To measure the CENP-E synthetic rate during the cell cycle, K562 cells at various phases of the cell cycle were obtained by centrifugal elutriation. An aliquot containing a total of 2.5×10^5 cells at the indicated cell cycle phase was removed, washed twice in prewarmed, methionine-free RPMI 1640 (Gibco Laboratories, Grand Island, NY), and incubated in 0.5 ml of the same medium for 30 min at 37°C. The cells were then pelleted and resuspended in 0.5 ml of medium, and 1 mCi of ^{35}S-TransLabel (ICN (Irvine, CA)) was added to each aliquot. After an additional 30-min incubation, the cells were washed three times in cold (4°C) PBS, and cell extracts prepared as outlined below.

For pulse-chase experiments, cells in the G1 phase of the cell cycle were obtained by elutriation and cells synchronized at the G1-S border were obtained by double-thymidine block. Aliquots of each cell population ($2.5 \times$

10^5 cells/time point) were obtained and labeled with 1 mCi of ^{35}S-Trans-Label. Cells were washed twice with complete media, resuspended in the same, and equal cell numbers were replated into parallel dishes. At the indicated times, cells were washed with cold PBS, and extracts for immunoprecipitation were prepared by incubating the washed cells in 100 μl of lysis buffer (50 mM Tris-HCl, pH 8.0, 150 mM NaCl, 1% Triton X-100, 0.5% Na-deoxycholate) containing protease inhibitors (10 μg/ml E-64, 1 μg/ml *N*-tosyl-L-phenylalanine chloromethyl ketone, 0.1 μg/ml Pepstatin, 50 μg/ml *N*-tosyl-L-lysine chloromethyl ketone, 50 μg/ml antipain, 40 μg/ml PMSF, 12 μg/ml phosphoamidon, 6 μg/ml leupeptin, 6 μg/ml aprotinin; all inhibitors were purchased from Boehringer-Mannheim Corp. [Indianapolis, IN]). The extracts were then vortexed briefly and centrifuged (10 min/14,000 rpm at 4°C) to pellet the nuclei and other insoluble material. The level of ^{35}S incorporation in each of the extracts was determined by scintillation counting of the TCA-precipitable material after alkaline hydrolysis (Pelham and Jackson, 1976). For synthetic rate studies, a volume of cell extract containing 5×10^6 cpm was combined with 2 μl of pAb1 and lysis buffer (final vol 50 μl), and the tubes were placed on ice for 1 h. After this, 25 μl of a 50% (vol/vol) slurry of protein A–Sepharose beads (Pharmacia Fine Chemicals, Piscataway, NJ) diluted in PBS was added and the tubes were rotated in an end-over-end fashion at 4°C for 1 h. Subsequently, the beads were collected by centrifugation, washed extensively in RIPA buffer (50 mM Tris-HCl, pH 8.0, 150 mM NaCl, 1% Triton X-100, 0.5% Na-deoxycholate, 0.1% SDS, 1 mM EDTA, 100 μM PMSF) at 4°C, and finally boiled in 50 μl of SDS sample buffer. The entirety of each sample was then subjected to SDS-PAGE, and the gels were processed for fluorography.

RNA Analysis

Total cellular RNA was isolated from elutriated K562 cells using guanidine isothiocyanate as described (Sambrook et al., 1989). To track the presence of CENP-E mRNA in these samples nuclease S1 analysis was conducted as outlined by Yen et al. (1988). As a probe, a CENP-E cDNA clone (clone 11B [Yen et al., 1992]) in BlueScript KSII was digested with Cla I and a 3.0-kb fragment that contains 204 bp (nucleotide no. 98-302) of the CENP-E open reading frame was isolated. Subsequently, this DNA fragment was 5′ end-labeled with ^{32}P, hybridized to 100 μg of RNA isolated from the elutriated cell fractions, and following S1 digestion, the protected fragments were resolved on an 8% acrylamide, 7 M urea gel and visualized by autoradiography. Hpa II digested pBR322 fragments were used as size markers.

Expression and Purification of CENP-E Using a Baculovirus Expression System

The entirety of the CENP-E cDNA was originally isolated as seven overlapping cDNA clones (Yen et al., 1992). Subsequently, a full-length CENP-E cDNA clone was constructed using convenient internal restriction sites. After the creation this clone in BlueScript KS II cloning vector (Stratagene, La Jolla, CA), the full-length CENP-E cDNA was cloned as an 8.3-kb BamHI-SalI fragment into the baculovirus recombination/expression vector pVL 1393 (Invitrogen, San Diego, CA). The resultant plasmid (pVL CE 1-2663) was then co-transfected into Sf9 cells along with linearized baculovirus genomic DNA (Baculo-Gold) according to the manufacturer's specifications (PharMingen, San Diego, CA). Subsequently, recombinant baculovirus was purified by serial dilution and amplified. CENP-E expression in Sf9 cells infected with excess virus was highest 96 h after infection.

To obtain large quantities of recombinant CENP-E, 2×10^8 Sf9 cells were infected with $\sim 1 \times 10^9$ pfu of recombinant baculovirus. After 96 h the cells were harvested by centrifugation (5 min/2,000 rpm) and washed extensively in PBS. The cells were then lysed by sonication in column buffer (50 mM Tris-HCl, pH 7.5, 5 mM EDTA, 1 mM PMSF), the insoluble material was removed by centrifugation (10 min/14,000 rpm at 4°C), and soluble lysate was then applied to a Sephrose CL-4B column (bed volume ~150 ml) at a flow rate of 1 ml/5 min. Column fractions were assayed for CENP-E content by SDS-PAGE followed by Coomassie blue staining, and the CENP-E–enriched fractions were pooled. The absolute quantity of CENP-E in the partially purified fraction was determined to be 10 μg/ml by scanning densitometry (Ultroscan XL; Pharmacia Biotech, Piscataway, NJ) using purified skeletal muscle myosin as a standard.

Qantitation of Immunoprecipitations and Immunoblots

Signals from metabolically labeled proteins and immunoblots labeled with ^{125}I-protein A were quantified by phosphorimaging (Molecular Dynamics, Inc., Sunnyvale, CA). For quantitative immunoblot analysis, a standard curve of signal vs amount of CENP-E was obtained by analysis of a series of known amounts of CENP-E immunoblotted in parallel. For this, full-length CENP-E was partially purified from Sf9 cells infected with recombinant baculovirus as outlined above. Appropriate quantities of cell extracts and purified recombinant CENP-E were subjected to SDS-PAGE followed by electrotransfer to nitrocellulose sheets. All gels in a single assay were transferred in the same cassette to a single sheet of nitrocellulose to assure equal transfer of the cell extracts and standards. The resultant nitrocellulose sheet was then processed for immunoblot analysis as outlined above.

Immunofluorescence Microscopy

Nocodazole-arrested mitotic HeLa cells were harvested by shake-off as outlined above, rinsed extensively in nocodazole-free complete media, and was finally suspended in complete media supplemented with 5 μg/ml cytochalasin D. After incubation for various times, the cells were harvested by centrifugation, rinsed several times with PBS, and the cell suspension was then applied to poly-L-lysine–coated coverslips for 10 min at room temperature. Subsequently, the coverslips were rinsed in PBS, and the cells were fixed by emersion in cold (−20°C) methanol for 5 min. The cells were then incubated at 37°C sequentially with: (*a*) mAb 177 (1:10 dilution of culture supernatant), (*b*) biotinylated goat anti-mouse IgG (1:500 dilution; Kirkegaard & Perry Laboratories, Inc., Gaithersburg, MD), (*c*) Texas red–conjugated strepavidin (1:1,000 dilution; Vector Laboratories, Burlingame, CA) and (*d*) 0.1 μg/ml 4′,6′-diamidino-2-phenyl-indole (DAPI)[1]. Cells were rinsed extensively in PBS between each incubation, and all reagents were diluted in PBS/5% bovine serum albumin. Finally, the coverslips were mounted and viewed in an epifluorescence microscope (BH2; Olympus Corp., Lake Success, NY) and images were recorded on 35-mm film (TMAX, 400 ASA; Eastman Kodak).

Results

CENP-E Accumulates Progressively during the Cell Cycle

Previous work determined that cells in G1 and early S phase contained little detectable CENP-E, while the levels of this protein rose sharply during late S and G2/M (Yen et al., 1992). To demonstrate directly cell cycle–dependent accumulation of CENP-E, we used centrifugal elutriation of cultures of the human erythroleukemia cell line K562 (Fig. 1 *A*). Immunoblotting of equal protein loadings from extracts of elutriated cells that represent the breadth of the cell cycle revealed a progressive accumulation (Fig. 1, *B* and *C*). Phosphorimaging revealed a 10-fold increase in CENP-E level per cell between G1 and G2/M. This represents a minimum estimate of the magnitude of the change in CENP-E abundance across the cycle, since currently available methods do not allow for the isolation of cell populations synchronized at the very beginning of G1 and the very end of G2.

To determine the mechanism responsible for CENP-E accumulation, the synthetic rate of CENP-E was measured by immunoprecipitation after pulse labeling of K562 cells with [^{35}S]methionine/cysteine. Immunoprecipitation using a polyclonal antibody (pAb1) to a bacterially expressed portion of the CENP-E rod revealed that a single high molecular weight protein was specifically precipitated (Fig. 2 *A*, lanes *1* and *2*). This protein was unambiguously identified as CENP-E, not only because of its expected size, but also because its precipitation was blocked by competition with purified CENP-E (expressed by recombinant baculovirus, see Fig. 4 *B*). CENP-E was quantitatively immunoprecipitated under these conditions, since addition of 10-fold as

1. *Abbreviation used in this paper*: DAPI, 4′,6′-diamidino-2-phenyl-indole.

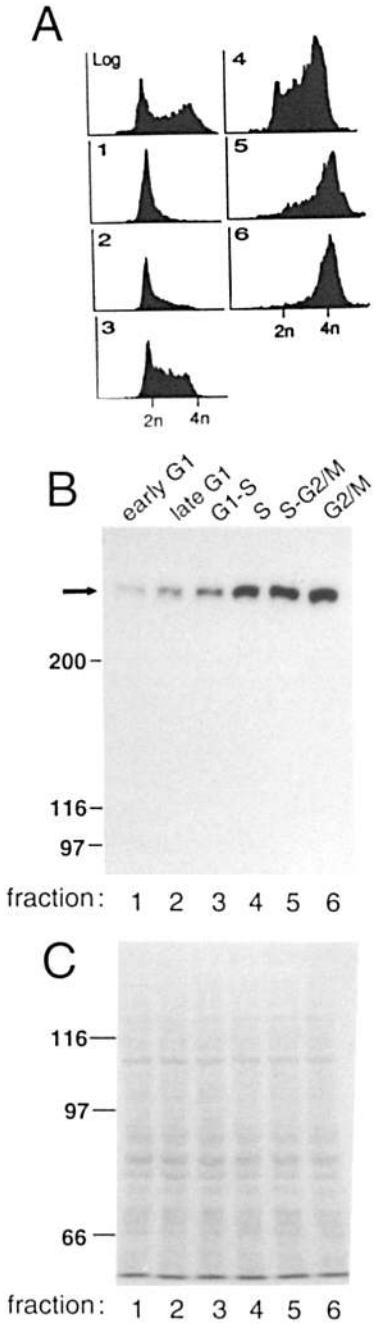

Figure 1. CENP-E accumulates progressively during the cell cycle. (*A*) Cytofluorographic analysis of K562 cells in exponential growth phase (Log) and elutriated cell fractions 1–6 (*abcissa*, DNA content; *ordinate*, nucleii content). (*B*) Extracts were made from the elutriated cell fractions 1–6, and equal protein loadings (50 μg/lane) from each fraction were subjected to immunoblot analysis with the anti-CENP-E antisera pAb1 (*arrow*, CENP-E). (*C*) Coomassie blue–stained gel of elutriated cell fractions to assure equal protein loadings. (Migration of molecular mass markers in kD is indicated.)

much cell extract yielded a proportionate increase in CENP-E precipitated, and immunoblot analysis of the supernatants revealed no detectable CENP-E in these fractions (data not shown). Immunoprecipitation after pulse-labeling of cells isolated by elutriation at various points in the cell cycle revealed that CENP-E was synthesized during the entirety of the cell cycle (Fig. 2 *B*), although phosphorimaging further showed that CENP-E synthetic rate in S and G2 was approximately twofold that in G1. Mechanistically, this modest increase in synthesis during the later stages of interphase corresponds to an increased mRNA content rather than a change in translation efficiency, since S1 nuclease analysis determined that the CENP-E mRNA level also increases approximately threefold from G1 to G2/M (Fig. 2 *C*).

To assess whether changes in protein stability contribute to cell-cycle dependent accumulation of CENP-E, K562 cells were metabolically labeled in G1 and chased for a total of 8.5 h (at which point ~30% of the cells had transitioned into S phase [data not shown]). Immunoprecipitation of CENP-E revealed a gradual loss (Fig. 3 *A*), corresponding to $t_{1/2}$ during G1 of ~6 h (Fig. 3 *C*). After pulse labeling of cells synchronized at the G1/S boundary (using double thymidine block), no diminution of CENP-E signal was observed during the entirety of the subsequent S and G2 phases (Fig. 3, *B* and *C*). Since we believe a 25% reduction (a loss that would require a half-life of 14 h for the combined 8 h S and G2 phases) would have been detectable, this establishes that CENP-E is stabilized to a cytoplasmic half-life of ≥14 h during late interphase.

CENP-E Undergoes Striking Loss after the Onset of Metaphase through a Cytokinesis-independent Mechanism

An initial qualitative pulse-chase experiment previously determined that CENP-E is lost as cells transition from M phase to G1 (Yen et al., 1992). To examine the mechanism responsible for this selective loss of CENP-E at the termination of mitosis, nearly pure populations of mitotic HeLa cells were collected via mitotic shake-off. Extracts were prepared immediately from some of these M phase cells. Additionally, extracts were made from others only after replating and incubation for 3 h, by which time virtually all of the cells had completed mitosis and had entered interphase. When these extracts were analyzed for CENP-E by immunoblotting, a strong signal for CENP-E was evident in the M phase extract made from 5×10^4 cells (Fig. 4 *A*, lane *1*), but no CENP-E was detected in the extract made from an equal number of early G1 cells (Fig. 4 *A*, lane *2*). To quantitatively measure the CENP-E content of cells in M phase vs G1, we isolated full-length CENP-E by using a baculovirus expression system (Fig. 4 *B*) and partially purifying CENP-E by gel filtration chromatography (Fig. 4 *B*, lanes *4* and *5*). CENP-E levels in M and G1 extracts were determined by phosphorimaging using quantitation standards provided by a dilution series of this recombinant CENP-E immunoblotted in parallel. This revealed M phase and G1 cell populations to contain 11.9 (±2.3) and 1.3 (±0.33) fg/cell, respectively, of CENP-E. By using the predicted molecular weight of CENP-E (312,000 Ds), this corresponds to ~22,000 CENP-E molecules/mitotic HeLa cell and ~2,400 molecules/cell in G1 (Fig. 4 *C*). Hence, when assessed on a per cell basis, CENP-E undergoes an ~10-fold loss between M phase and early G1 cell populations, a loss quantitatively similar to the 16-fold diminution measured for cyclin B in a parallel analysis of the same samples (not shown).

In an earlier report, CENP-E was shown to be restricted

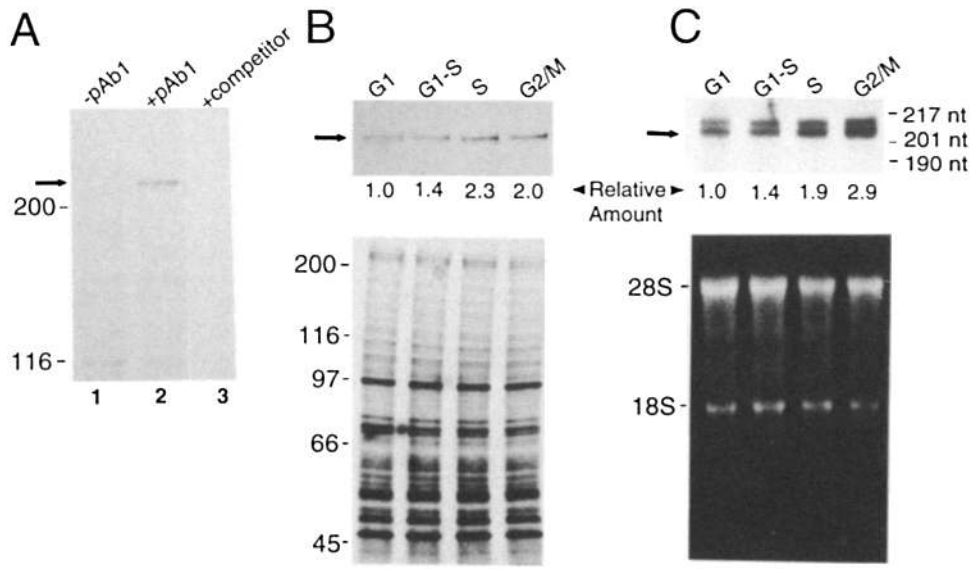

Figure 2. CENP-E is continually synthesized during the cell cycle. (*A*) Immunoprecipitation assays from metabolically labeled K562 cell extracts were conducted in the absence (lane *1*) and presence of pAb1 (lane *2*) and both pAb1 and purified recombinant CENP-E (50 ng) (lane *3*) followed by SDS-PAGE and fluorography. Note that a single high molecular weight protein (*arrow*) was specifically precipitated with pAb1, and that the precipitation of this protein was ablated by the addition of competitor. (*B*) Elutriated K562 cells at the indicated points in the cell cycle were metabolically labeled and CENP-E immunoprecipitated from equal cpm from these extracts (2×10^5) with pAb1. (*Upper panel*) Autoradiogram of precipitated material, arrow marks presence of CENP-E; the relative abundance of the immunoprecipitated CENP-E in each fraction is noted. (*Lower panel*) 3×10^4 cpm from each of the extracts were assayed to assure that equal counts from each of the extracts were assayed. (*C*) Total RNA from elutriated K562 cells (100 μg/fraction) was subjected to S1 analysis to assess CENP-E mRNA levels. (*Upper panel*) Autoradiogram of protected fragments (*arrow*); the relative abundance of the 204 nucleotide (*nt*) protected fragment in each fraction is noted. (*Lower panel*) Total RNA from each of the cell fractions (2.5 μg/lane) was subjected to agarose gel electrophoresis followed by staining with ethidium bromide to assure equality of RNA assayed per fraction. The migration of the 28S and 18S rRNAs are indicated.

to the midbody during the later stages of mitosis (Yen et al., 1991). This observation, when combined with the finding that in the human cell line D-98S the midbody is discarded at the conclusion of cytokinesis (Mullins and Biesele, 1973, 1977), led to a working hypothesis that CENP-E sequestration to the midbody and subsequent loss of this structure represented the underlying mechanism responsible for CENP-E loss during the transition from mitosis to interphase. Since this proposed mechanism of loss requires cytokinesis, we tested it directly by comparing CENP-E levels in cells transiting from M to G1 in the presence or absence of cytokinesis. This was possible, since actin-disrupting cytochalasins have been shown to inhibit cytokinesis (Carter, 1967; Schroeder, 1970) without affecting cell cycle advance.

In an initial experiment, HeLa cells were blocked at prometaphase using the reversible microtubule inhibitor nocodazole, the nocodazole was removed, and the mitotic cells were replated in the presence or absence of 5 μg/ml cytochalasin D. Immunofluorescence microscopy confirmed that, as expected, the cells were arrested in a prometaphase-like state with condensed chromatin and CENP-E (visualized with the anti–CENP-E monoclonal antibody mAb 177 [Yen et al., 1991]) localized as discrete dots within the chromatin mass (Fig. 5 *A*). Within 1 h after the simultaneous release of the nocodazole block and addition of cytochalasin D, the majority of the cells had chromosomes aligned along the metaphase plate (metaphase cells) or chromosomes in the process of translocation towards opposite poles (anaphase cells) (Fig. 5, *B* and *C*, respectively). Metaphase cells revealed CENP-E immunoreactivity as distinct dots colocalized with the chromosomes (Fig. 5 *B*), whereas by anaphase CENP-E had relocalized to the interzonal microtubules of the spindle (Fig. 5 *C*). Within 2 h after removal of the nocodazole arrest, the majority of cells cultured in the absence of cytochalasin D had completed cell division (data not shown). At the same time point, an equal proportion of

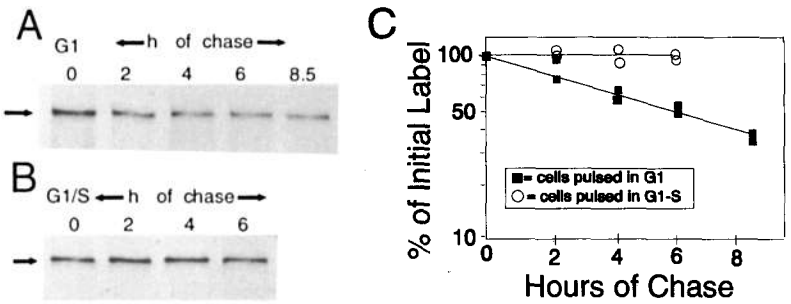

Figure 3. Stability of the CENP-E polypeptide during the cell cycle. Pulse-chase analysis on K562 cells at the indicated points in the cell cycle was conducted. Subsequently, extracts were prepared and immunoprecipitation of CENP-E, followed by SDS-PAGE and fluorography, was performed. (*A*) Pulse-chase analysis of K562 cells isolated in the G1 phase of the cell cycle by elutriation. (*B*) Pulse-chase analysis of K562 cells synchronized at the G1/S border by a double-thymidine block (*arrow*, CENP-E). (*C*) Graphical depiction of the measured CENP-E signal values obtained from two pulse-chase experiments.

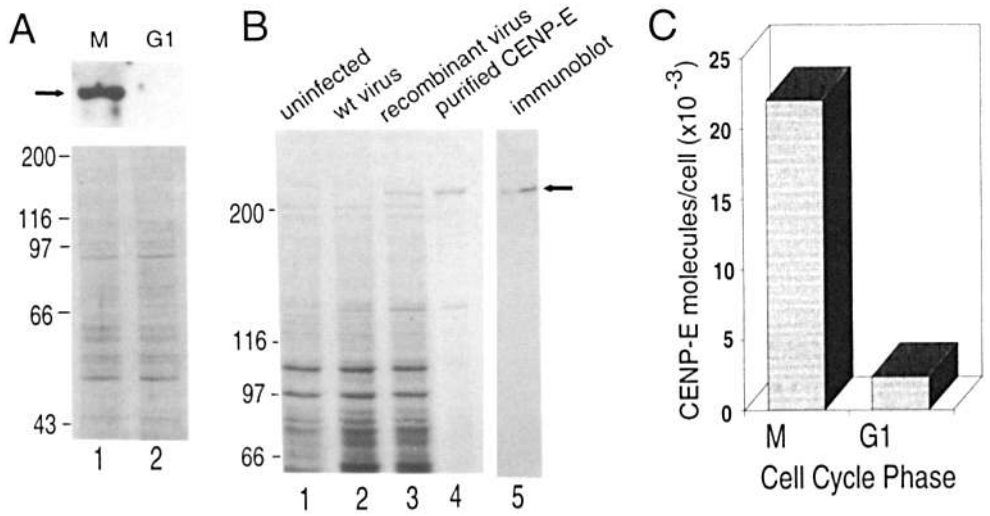

Figure 4. CENP-E undergoes a quantitative 10-fold loss as cells transition from mitosis to interphase. (*A*) Extracts of mitotic HeLa cells (lane *1*) and cells that have completed mitosis and reentered interphase (lane *2*) were analyzed. (*Upper panel*) Extracts prepared from 5×10^4 cells of each population were subjected to immunoblot analysis with pAbl, CENP-E is noted (*arrow*). (*Lower panel*) Coomassie blue–stained gel of equal cell numbers of each cell population. (*B*) Extracts (50 μg/lane) from uninfected Sf9 cells (lane *1*), cells infected with wild type (lane *2*), and recombinant baculovirus expressing the full-length CENP-E molecule (lane *3*), as well as a preparation of purified recombinant CENP-E (lane *4*, 10 μg), were subjected to SDS-PAGE followed by Coomassie blue staining. (Lane *5*) Immunoblot of purified CENP-E fraction (500 ng) with pAbl. Migration of expressed CENP-E is noted (*arrow*). (*C*) CENP-E content in M and G1 extracts was measured by quantitative immunoblotting as outlined in Materials and Methods. Shown is a graphical depiction of the calculated values for CENP-E molecules/cell in M and G1.

cells cultured in the presence of cytochalasin D progressed into G1 but without undergoing cytokinesis, as demonstrated by the presence of two well-formed nuclei with decondensed chromatin contained within the borders of a single cell (Fig. 5, *D* and *E*). Staining of these cells with lamin antisera confirmed the reassembly of a nuclear lamina in each nucleus (data not shown). Despite the inhibition of cell division, indirect immunofluorescence failed to detect CENP-E in binucleate cells (Fig. 5, *D* and *E*, *arrowed cells*), although it was readily observable in the few cells still in mitosis (Fig. 5 *E*, *arrowhead*). As these observations correlate exactly with the previously determined localization of CENP-E in non–drug treated cells (Yen et al., 1991) and nocodazole-arrested cells released from the drug but replated in the absence of cytochalasin D (data not shown), we conclude that the cytochalasin D–dependent inhibition of cytokinesis does not affect the localization of CENP-E during mitotic progression. However, the subsequent apparent loss of CENP-E in cells that have completed mitosis without undergoing cytokinesis is inconsistent with CENP-E loss requiring CENP-E sequestration to and loss with the midbody.

To prove directly that the diminished fluorescence of CENP-E as cells progress from M to G1 reflected actual polypeptide loss in the absence of cytokinesis, extracts were prepared from cells at various times after release from nocodazole arrest. Immunoblotting revealed clearly that most CENP-E was lost during a 2-h period after release from the nocodazole block, regardless of whether cytochalasin D was present (Fig. 6, *A* and *B*, *top panels*). CENP-E loss mirrored that seen for cyclin B (Fig. 6, *A* and *B*, *middle panels*), whose degradation during mitotic progression in invertebrate oocyte systems is known not to require cytokinesis (e.g., Standart et al., 1987; Hunt et al., 1992). Also like cyclin B, loss of CENP-E requires postprometaphase mitotic progression (Fig. 6 *C*, *top and middle panels*), since in mitotically arrested cells replated in the presence of colchicine, both CENP-E and cyclin B levels remained unchanged over a subsequent 2-h period. Additionally, immunoblot analysis of these extracts with an antitubulin antibody revealed that the tubulin levels remain constant in all extracts, confirming the uniformity of the protein loadings and the absence of generalized proteolysis (Fig. 6, *A–C*, *bottom panels*).

To determine whether CENP-E degradation coincides temporally with destruction of cyclin B, CENP-E and cyclin B levels were quantified during mitotic progression after release from nocodazole-induced prometaphase arrest (Fig. 7). This revealed that ~60% of the cyclin B was lost 1 h after the release of the nocodazole block, and that degradation continued steadily during a 2-h time period. While CENP-E undergoes a comparable degree of loss during the same time period, loss of this polypeptide initiates only after a 1-h lag.

Overall, we conclude that CENP-E is selectively lost through a degradative pathway that initiates in late anaphase/telophase.

Discussion

To earlier identification of CENP-E to be the only kinesin-like, putative microtubule-dependent motor presently known to associate with kinetochores during mitotic chromosome movements, we have now shown that CENP-E is also one of only a handful of mammalian proteins whose accumulation and loss is known to be coupled to cell cycle progression. Further, although a modest increase in CENP-E synthesis is seen between G1 and G2, we have found in both interphase and mitosis that accumulation and loss results primarily from changes in the rate of CENP-E degradation, rather than the rate of synthesis. Moderately unstable during G1 ($t_{1/2}$ of ~6 h), CENP-E is completely stabilized during S/G2 and the stages of mitosis through metaphase. However, after the anaphase transition, CENP-E is destined for inactivation at the terminal phases of mitosis through parallel pathways that

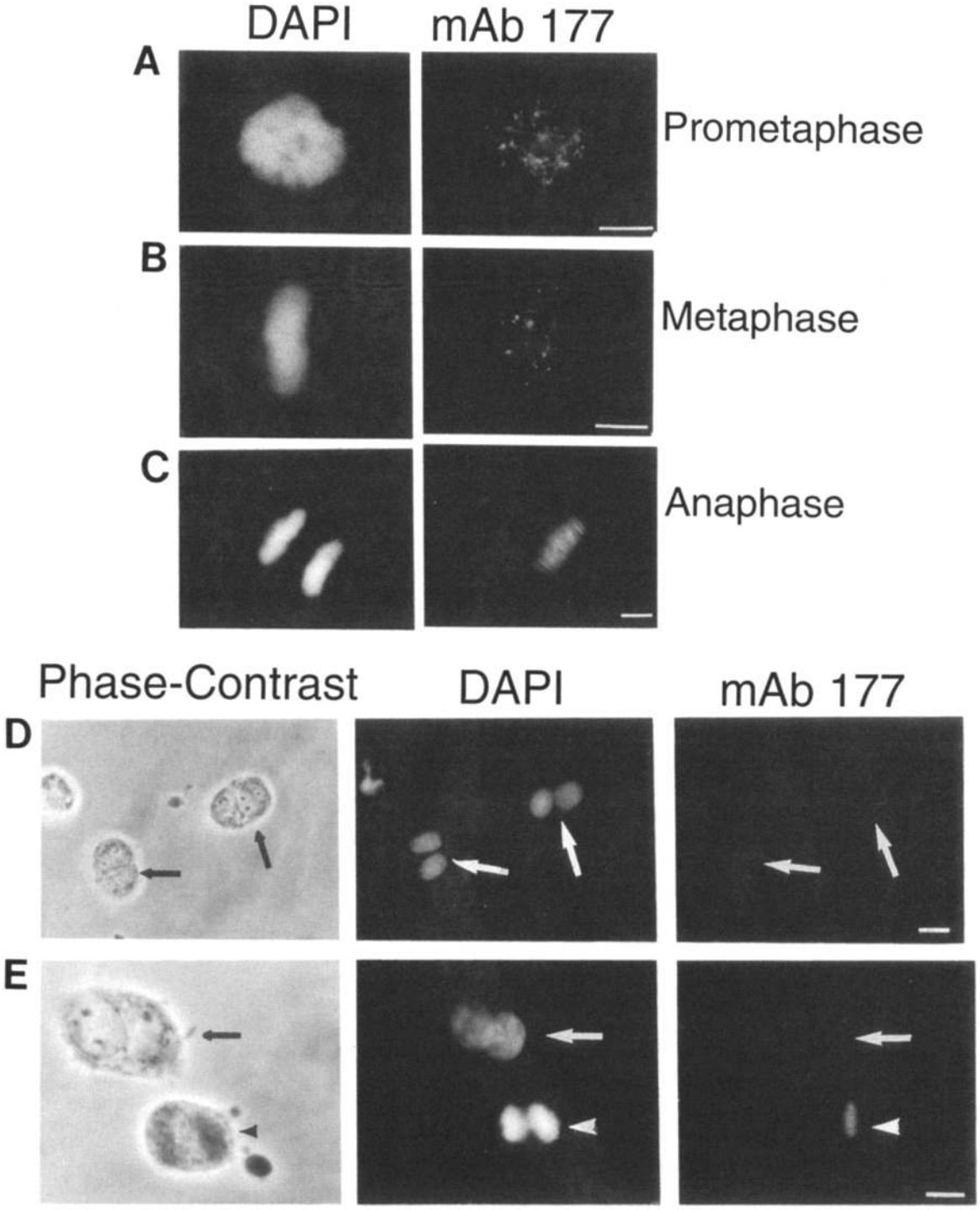

Figure 5. Cytochalasin D treatment of mitotic HeLa cells blocks cytokinesis but exerts no effect on CENP-E localization during mitotic progession. Mitotically arrested HeLa cells (nocodazole block) were collected and replated in the presence of cytochalasin D (5 μg/ml). At the indicated times, cells were fixed and stained with DAPI to visualize DNA and with mAb 177 to visualize CENP-E. (*A*) O h after release from nocodazole. (*B*) Cell in metaphase 1 h after release from nocodazole. (*C*) Cell in anaphase 1 h after release from nocodazole. (*D* and *E*) Cells 2 h after release from block. (*Arrows*, nuclei present within bi-nucleate cells; *arrowhead*, cell in anaphase). Scale bar, 5 μm, *A* and *C*; 10 μm, *D* and *E*.

sequester it to the developing midbody and selectively degrade it.

Combining the measured synthetic rates in G1 vs S and G2, the pseudo–first-order decay during G1, and the rapid degradation of almost all CENP-E at the later stages of M yields the pattern for CENP-E accumulation shown in Fig. 8 *A*. CENP-E accumulates primarily in G2 as a result of selective stabilization and a modest increase in synthesis. CENP-E polypeptide accumulation and loss is reminiscent of that initially described for cyclins A and B, proteins first

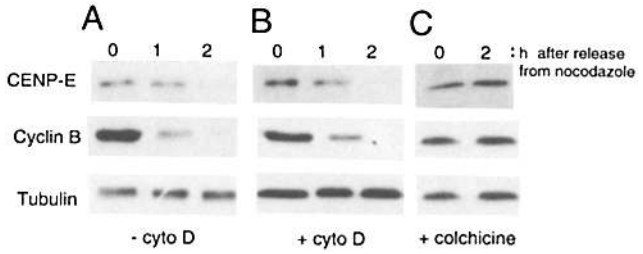

Figure 6. The inhibition of cytokinesis with cytochalasin D exerts no effect on the loss of CENP-E during mitotic progression. HeLa cells blocked in mitosis with nocodazole were collected by mitotic shake-off. (*A*) Cells replated in the absence of cytochalasin D (DMSO was added to 0.1%). (*B*) Cells replated in the presence of cytochalasin D (5 μg/ml). (*C*) Cells replated in the presence of colchicine (1 μM). Extracts from treated cells were prepared at the indicated time points, and immunoblot analysis for the indicated proteins was performed. All lanes probed for CENP-E loaded at 35 μg total protein/lane, 50 μg/lane for cyclin B, and 10 μg/lane for tubulin.

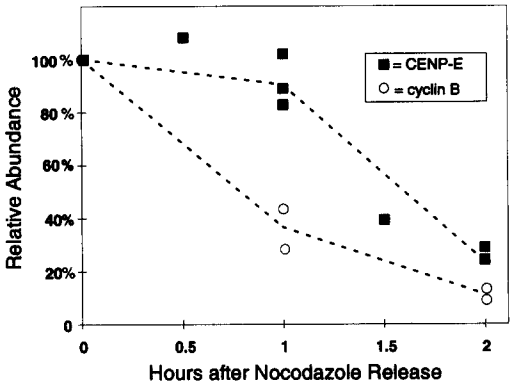

Figure 7. Kinetics of CENP-E and cyclin B loss after release from nocodazole. Mitotically blocked (nocodazole) HeLa cells were collected by mitotic shake and replated in the absence of the drug. Extracts were formed at the indicated time points and quantitative immunoblot analysis was performed. Graphical representation of measured immunoblot signals is displayed.

discovered as a consequence of their oscillatory accumulation and destruction in invertebrate oocytes after fertilization (Evans et al., 1983; Swenson et al., 1986; Standart et al., 1987). The cyclins are continuously synthesized between cell divisions and are rapidly degraded near the end of mitosis in invertebrate embryos (Evans et al., 1983; Swenson et al., 1986; Standart et al., 1987). In human cells, cyclin B accumulates sharply in G2 (an increase arising from a four-fold elevation in cyclin mRNA levels), peaks in early M, and then plummets in abundance by the end of cell division (Pines and Hunter, 1989). Although the G2 increase in cyclin B relies more heavily on increased mRNA abundance, the pattern of accumulation of both CENP-E and cyclin B are similar overall, accumulating primarily in G2 and rapidly degraded during the later portion of M phase.

The degradation of CENP-E, combined with three earlier examples (cyclin A, cyclin B, and as yet unidentified component(s) degraded at the metaphase/anaphase transition; see below) defines a cascade of at least four temporally regulated proteolytic steps during mitosis (outlined schematically in Fig. 8 *B*). The earliest of these is degradation of cyclin A, whose loss clearly precedes degradation of cyclin B both in embryonic systems (Minshull et al., 1989*b*, 1990; Luca and Ruderman, 1989; Lehner and O'Farrell, 1990; Hunt et al., 1992) and human cells (Pines and Hunter, 1990). Since degradation of cyclin A but not cyclin B proceeds normally in mitotic cells treated with microtubule disrupting agents (Minshull et al., 1989*b*; Hunt et al., 1992; Edgar et al., 1994), and cyclin B but not cyclin A can be detected in metaphase cells of early *Drosophila* embryos (Lehner and

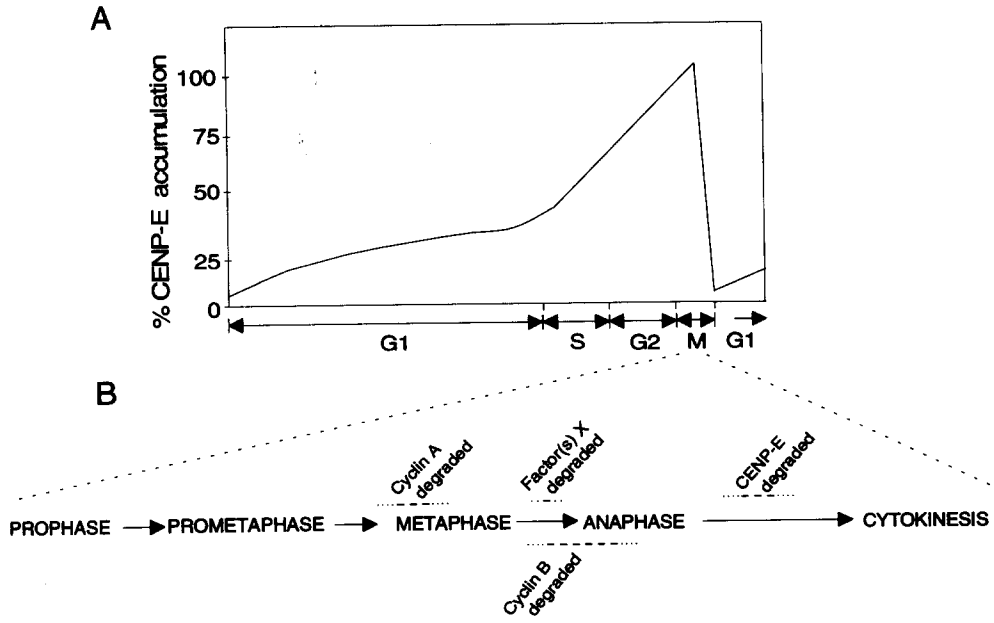

Figure 8. Kinetics of CENP-E accumulation across the cell cycle and timing of degradation during mitosis. (*A*) CENP-E accumulation during the cell cycle calculated from measured synthetic and degradation rates. (*B*) The morphological stages of mitosis are illustrated along with the established sequence and timing of the degradation of cyclin A, cyclin B, and CENP-E during mitotic progression. The proteolytic substrate(s) whose degradation triggers the metaphase to anaphase transition is denoted as Factor(s) X.

O'Farrell, 1990), cyclin A must be degraded before the metaphase/anaphase transition. In contrast, (and contrary to a widely accepted view, e.g., Murray and Kirschner, 1989*a*), it is now clear that cyclin B degradation occurs after the metaphase to anaphase transition. This was initially shown by Surana et al. (1993), who showed that at the restrictive temperature, *Saccharomyces cervisiae*, which harbor a temperature-sensitive *cdc15*, progress into mitosis and subsequently arrest in late anaphase/telophase, but with undiminished cyclin B levels. This finding was confirmed and extended using frog egg extracts that can be manipulated to complete the cell cycle in vitro, including assembly of mitotic spindles, anaphase chromosome segregation, and reformation of normal interphase nuclei. With this approach, Holloway et al. (1993) showed that anaphase chromosome movement can occur without cyclin B degradation or diminution of $p34^{CDC2}$ activity. Despite this, anaphase movement was blocked by addition of inhibitors of ubiquitin-mediated proteolysis. Taken together, these findings indicate that cyclin B degradation is not the trigger for initiation of anaphase, and that ubiquitin-dependent proteolysis of a substrate(s) other than cyclin B is required for the execution of the metaphase to anaphase transition. It remains unclear if cyclin B degradation occurs contemporaneously with the beginning of anaphase or at a later point in mitotic progression. As we have shown here, CENP-E degradation represents a further proteolytic step that initiates after cyclin B.

While only a handful of other proteins are known to undergo cell cycle–dependent accumulation, there may be further proteolytic steps yet to be uncovered. One obvious example is thymidine kinase, which is reduced in abundance by 15-fold at the terminal phases of mitosis (Sherley and Kelly, 1988), although the exact timing of degradation is unknown. Changes in abundance have also been reported for two other chromosomal proteins, topoisomerase II (Heck et al., 1988) and the INCENPs, a family of proteins that lie between sister chromatids at metaphase, lose their association with chromosomes just before or just after sister chromatid separation, and ultimately associate with the midbody (Cooke et al., 1987). For topoisomerase II, abundance changes only modestly (~50% diminution; Heck et al., 1988), but the INCENPs mirror the behavior of CENP-E in that they accumulate during S/G2 and are apparently lost by sequestration to the developing midbody (Cooke et al., 1987). It is not yet known whether, like CENP-E, the INCENPs are also degraded.

As to the mechanism(s) mediating the events of this proteolytic cascade, ubiquitin-mediated proteolysis has been shown to be responsible for the degradation of the cyclins (Glotzer et al., 1991; Hershko et al., 1991). It should also be noted that active cyclin B/$p34^{CDC2}$ complexes are necessary to activate the cyclin destruction pathway(s) (Luca et al., 1991). Since CENP-E contains a sequence ($_{967}$RNALESLKQ$_{975}$) highly similar to the RAALAVLKS "destruction box" proposed to mediate the ubiquitin-dependent proteolysis of human cyclin A (Glotzer et al., 1991), it seems plausible that CENP-E degradation may also be mediated by a ubiquitin-dependent mechanism. Alternatively, CENP-E contains two regions (residues 459–489 and 2480–2488) with strong homology to PEST sequences (PEST-FIND scores of 5.8 and 1.7, respectively [Rogers et al., 1986]). Since PEST sequences, which are rich in proline (P), glutamic acid (E), serine (S), and threonine (T) residues, have been shown to be responsible for the rapid intracellular degradation of a variety of proteins (Rogers et al., 1986; Rechsteiner, 1990), CENP-E degradation may be mediated through such motifs.

Whatever the mechanism(s) of degradation of proteins are at each step of the cascade, it is clear that a series of timed proteolytic steps are key events during mitotic progression.

We thank Drs. Mike Kaufmann and Thomas Kelly (Department of Molecular Biology and Genetics, Johns Hopkins University School of Medicine) for their advice on cell elutriations, and Dr. Ruth Muschel (Department of Pathology, University of Pennsylvania) for her generous gift of anti-cyclin B antisera. K. D. Brown was supported by a postdoctoral fellowship (PF-3976) from the American Cancer Society. T. J. Yen is a Lucille P. Markey scholar.

This work has been supported by a grant (GM 29513) to D. W. Cleveland from the National Institutes of Health.

Received for publication 3 January 1994 and in revised form 31 March 1994.

References

Blose, S. H., D. I. Meltzer, and J. R. Feramisco. 1984. 10-nm filaments are induced to collapse in living cells microinjected with monoclonal and polyclonal antibodies against tubulin. *J. Cell Biol.* 98:847–858.

Carter, S. B. 1967. Effects of cytochalasins on mammalian cells. *Nature (Lond.).* 213:261–264.

Cooke, C. A., M. M. S. Heck, and W. C. Earnshaw. 1987. The inner centromere protein (INCENP) antigens: movement from inner centromere to midbody during mitosis. *J. Cell Biol.* 105:2053–2067.

Edgar, B. A., F. Sprenger, R. J. Duronio, P. Leopold, and P. H. O'Farrell. 1994. Distinct molecular mechanisms regulate cell cycle timing at successive stages of Drosophila embryogenesis. *Genes & Dev.* 8:440–452.

Endow, S. A. 1991. The emerging kinesin family of microtubule motor proteins. *TIBS (Trends Biochem. Sci.)* 16:221–225.

Euteneur, U., and J. R. McIntosh. 1981. Structural polarity of kinetochore microtubules in PtK1 cells. *J. Cell Biol.* 89:338–345.

Evans, T., E. T. Rosenthal, J. Youngblom, D. Distel, and T. Hunt. 1983. Cyclin: a protein specified by maternal mRNA in sea urchin eggs that is destroyed at each cleavage division. *Cell.* 33:389–396.

Gallant, P., and E. A. Nigg. 1992. Cyclin B2 undergoes cell cycle dependent nuclear translocation and, when expressed as a nondestructable mutant, causes mitotic arrest in HeLa cells. *J. Cell Biol.* 117:214–224.

Glotzer, M., A. W. Murray, and M. W. Kirschner. 1991. Cyclin is degraded by the ubiquitin pathway. *Nature (Lond.).* 349:132–138.

Gorbsky, G. J., P. J. Sammak, and G. G. Borisy. 1987. Chromosomes move poleward in anaphase along stationary microtubules that coordinately disassemble from their kinetochore ends. *J. Cell Biol.* 104:9–18.

Heck, M. M. S., W. N. Hittleman, and W. C. Earnshaw. 1988. Diffential expression of DNA topoisomerases I and II during the eukaryotic cell cycle. *Proc. Natl. Acad. Sci. USA.* 85:1086–1090.

Hershko, A., D. Ganoth, J. Pehrson, R. E. Palazzo, and L. H. Cohen. 1991. Methylated ubiuitin inhibits cyclin degradation in clam embryo extracts. *J. Biol. Chem.* 266:16376–16379.

Holloway, S. L., M. Glotzer, R. W. King, and A. W. Murray. 1993. Anaphase is initiated by proteolysis rather than by the inactivation of maturation-promoting factor. *Cell.* 73:1393–1402.

Hunt, T., F. C. Luca, and J. V. Ruderman. 1992. The requirements for protein synthesis and degradation, and the control of destruction of cyclins A and B in the meiotic and mitotic cell cycles of the clam embryo. *J. Cell Biol.* 116:707–724.

Hyman, A. A., and T. J. Mitchison. 1991. Two different microtubule-based motor activities with pposite polarities in kinetochores. *Nature (Lond.).* 351:206–211.

Kauffman, M. G., S. J. Noga, T. J. Kelly, and A. D. Donnenberg. 1990. Isolation of cell cycle fractions by counterflow centrifugal elutriation. *Anal. Biochem.* 191:41–46.

Koshland, D., T. J. Mitchison, and M. W. Kirschner. 1988. Polewards chromosome movement driven by microtubule depolymerization in vitro. *Nature (Lond.).* 331:499–501.

Laemmli, U. K. 1970. Cleavage of structural proteins during the assembly of the bacteriophage T4. *Nature (Lond.).* 337:650–655.

Lehner, C. F., and P. H. O'Farrell. 1990. The roles of drosophila cyclins A and B in mitotic control. *Cell.* 61:535–547.

Luca, F. C., and J. V. Ruderman. 1989. Control of programmed cyclin destruction in a cell-free system. *J. Cell Biol.* 109:1895-1909.

Luca, F. C., E. K. Shibuya, C. E. Dohrmann, and J. V. Ruderman. 1991. Both cyclin AΔ60 and BΔ97 are stable and arrest cells in M-phase, but only BΔ97 turns on cyclin destruction. *EMBO (Eur. Mol. Biol. Organ.) J.* 10:4311-4320.

Minshull, J., J. J. Blow, and T. Hunt. 1989*a*. Translation of cyclin mRNA is necessary for extracts of activated *Xenopus* eggs to enter mitosis. *Cell.* 56:947-956.

Minshull, J., J. Pines, R. Golsteyn, N. Standart, S. Mackie, A. Colman, J. Blow, J. V. Ruderman, M. Wu, and T. Hunt. 1989*b*. The control of cyclin synthesis, modification and destruction in the control of cell division. *J. Cell Sci. Suppl.* 12:77-97.

Minshull, J., R. Golsteyn, C. S. Hill, and T. Hunt. 1990. The A- and B-type cyclin-associated cdc2 kinases in *Xenopus* turn on and off at different times in the cell cycle. *EMBO (Eur. Mol. Biol. Organ.) J.* 9:2865-2875.

Mitchison, T. J., and M. W. Kirschner. 1985. Properties of the kinetochore in vitro. II. Microtubule capture and ATP translocation. *J. Cell Biol.* 101:767-777.

Mullins, J. M., and J. J. Biesele. 1973. Cytokinetic activities in a human cell line: the midbody and intracellular bridge. *Tissue & Cell.* 5:47-61.

Mullins, J. M., and J. J. Biesele. 1977. Terminal phase of cytokinesis in D-98S cells. *J. Cell Biol.* 73:672-684.

Murray, A. W., and M. W. Kirschner. 1989*a*. Dominoes and clocks; the union of two views of the cell cycle. *Science (Wash. DC).* 246:614-621.

Murray, A. W., and M. W. Kirschner. 1989*b*. Cyclin synthesis drives the early embryonic cell cycle. *Nature (Lond.).* 339:275-280.

Murray, A. W., M. J. Solomon, and M. W. Kirschner. 1989. The role of cyclin synthesis and degradation in the control of maturation promoting factor activity. *Nature (Lond.).* 339:280-286.

Muschel, R. J., H. B. Zhang, and W. G. McKenna. 1993. Differential effect of ionizing radiation on the expression of cyclin A and cyclin B in HeLa cells. *Cancer Res.* 53:1128-1135.

Nicklas, R. B. 1989. The motor for poleward chromosome movement in anaphase is in or near the kinetochore. *J. Cell Biol.* 109:2245-2255.

Norbury, C., and P. Nurse. 1992. Animal cell cycles and their control. *Annu. Rev. Biochem.* 61:441-470.

Pelham, H. R. B., and R. J. Jackson. 1976. An efficient mRNA-dependent translation system from reticulocyte lysates. *Eur. J. Biochem.* 67:247-256.

Pines, J., and T. Hunter. 1989. Isolation of a human cyclin cDNA: evidence for cyclin mRNA and protein regulation in the cell cycle and for interaction with p34cdc2. *Cell.* 58:833-846.

Pines, J., and T. Hunter. 1990. Human cyclin A is adenovirus E1A-associated protein p60 and behaves differently from cyclin B. *Nature (Lond.).* 346:760-763.

Rechsteiner, M. 1990. PEST sequences are signals for rapid intracellular proteolysis. *Sem. Cell Biol.* 1:433-440.

Reider, C. L., and S. P. Alexander. 1990. Kinetochores are transported poleward along a single astral microtubule during chromosome attachment to the spindle in new lung cells. *J. Cell Biol.* 110:81-95.

Rogers, S., R. Wells, and M. Rechsteiner. 1986. Amino acid sequences common to rapidly degraded proteins: the PEST hypothesis. *Science (Wash. DC).* 234:364-368.

Sambrook, J., E. F. Fritsch, and T. Miniatis. 1989. Molecular cloning: A Laboratory Manual. 2nd ed. Cold Spring Harbor Laboratory Press, Plainview, NY. pp. 7.6-7.9.

Schroeder, T. E. 1970. The contractile ring. I. Fine structure of dividing mammalian (HeLa) cells and the effects of cytochalasin B. *Z. Zellforsch. Mikrosk. Anat.* 109:431-449.

Sherley, J. L., and T. J. Kelly. 1988. Regulation of human thymidine kinase during the cell cycle. *J. Biol. Chem.* 263:8350-8358.

Skoufias, D. A., and J. M. Scholey. 1993. Cytoplasmic microtubule-based motor proteins. *Curr. Opin. Cell Biol.* 5:95-104.

Smith, P. K., P. I. Krhon, G. T. Hermanson, A. K. Malia, F. H. Gartner, M. D. Provenzaus, E. K. Fujimoto, N. M. Goeke, B. J. Olson, and D. C. Klenk. 1985. Measurement of protein using bicinchonic acid. *Anal. Biochem.* 150:76-85.

Standart, N., J. Minshull, J. Pines, and T. Hunt. 1987. Cyclin synthesis, modification and destruction during meiotic maturation of the starfish oocyte. *Dev. Biol.* 124:248-258.

Surana, U., A. Amon, C. Dowzer, J. McGrew, B. Byers, and K. Nasmyth. 1993. Destruction of the CDC228/CLB mitotic kinase is not required for the metaphase to anaphase transition in budding yeast. *EMBO (Eur. Mol. Biol. J.) J.* 12:1969-1978.

Swenson, K. I., K. M. Farrell, and J. V. Ruderman. 1986. The clam embryo protein cyclin A induces entry into M phase and the resumption of meiosis in Xenopus oocytes. *Cell.* 47:861-870.

Towbin, H., T. Staehelin, and J. Gordon. 1979. Electrophoretic transfer of proteins from polyacrylamide gels to nitrocellulose sheets: procedure and some applications. *Proc. Natl. Acad. Sci. USA.* 76:4350-4354.

van der Velden, H. W., and M. J. Lohka. 1993. Mitotic arrest caused by the amino terminus of *Xenopus* cyclin B2. *Mol. Cell Biol.* 13:1480-1488.

Westendorf, J. M., K. I. Swenson, and J. V. Ruderman. 1989. The role of cyclin B in meiosis I. *J. Cell Biol.* 108:1431-1444.

Yen, T. J., D. A Gay, J. S. Pachter, and D. W. Cleveland. 1988. Autoregulated changes in the stability of polyribosome-bound β-tubulin mRNAs are specified by the first thirteen translated nucleotides. *Mol. Cell Biol.* 8:1224-1235.

Yen, T. J., D. A. Compton, D. Wise, R. P. Zinkowski, B. R. Brinkley, W. C. Earnshaw, and D. W. Cleveland. 1991. CENP-E, a human centromere associated protein required for progression from metaphase to anaphase. *EMBO (Eur. Mol. Biol. J.) J.* 10:1245-1254.

Yen, T. J., G. Li, B. T. Schaar, I. Szilak, and D. W. Cleveland. 1992. CENP-E is a putative kinetochore motor that accumulates just before mitosis. *Nature (Lond.).* 359:536-539.